The C-Terminal Region of the Stalk Domain of Ubiquitous Human Kinesin Heavy Chain Contains the Binding Site for Kinesin Light Chain†

Russell J. Diefenbach,*,‡ Joel P. Mackay,§ Patricia J. Armati,|| and Anthony L. Cunningham‡

Centre for Virus Research, Westmead Institutes of Health Research, Westmead Hospital, Westmead, NSW 2145, Australia, and Department of Biochemistry and School of Biological Sciences, University of Sydney, NSW 2006, Australia

Received May 18, 1998; Revised Manuscript Received September 21, 1998

ABSTRACT: The motor protein kinesin is a heterotetramer composed of two heavy chains of ∼120 kDa and two light chains of ∼65 kDa protein. Kinesin motor activity is dependent on the presence of ATP and microtubules. The kinesin light chain-binding site in human kinesin heavy chain was determined by reconstituting in vitro a complex of recombinant heavy and light chains. The proteins expressed in bacteria included oligohistidine-tagged fragments of human ubiquitous kinesin heavy chain, spanning most of the stalk and all of the tail domain (amino acids 555−963); and untagged, essentially full-length human kinesin light chain (4−569) along with N-terminal (4−363) and C-terminal (364−569) light chain fragments. Heavy chain fragments were attached to Ni^{2+}-charged beads and incubated with untagged light chain fragments. Analysis of eluted complexes by SDS−PAGE and immunoblotting mapped the light chain-binding site in heavy chain to amino acids 771−813, a region close to the C-terminal end of the heavy chain stalk domain. In addition, only the full-length and N-terminal kinesin light chain fragments bound to this heavy chain region. Within this heavy chain region are four highly conserved contiguous heptad repeats (775−802) which are predicted to form a tight α-helical coiled-coil interaction with the heptad repeat-containing N-terminus of the light chain, in particular region 106−152 of human light chain. This predicted hydrophobic, α-helical coiled-coil interaction is supported by both circular dichroism spectroscopy of the recombinant kinesin heavy chain fragment 771−963, which displays an α-helical content of 70%, and the resistance of the heavy/light chain interaction to high salt (0.5 M).

Kinesin is an ATP-dependent, microtubule-binding motor protein first identified in squid axoplasm (*1*). It has been purified from a variety of sources and shown in vitro to exhibit both microtubule-activated ATPase activity and fast (∼0.6 μm/s) plus end directed microtubule-based transport of cargo such as latex beads (*1*−*7*). On the basis of these observations, it was proposed that kinesin is the in vivo motor protein responsible for fast anterograde (plus end-directed) transport of axonal vesicles along microtubules (*2*, *3*). In support of this proposal, monoclonal antibodies to kinesin heavy and light chain were shown to inhibit both anterograde and retrograde fast axonal transport in squid axoplasm and to demonstrate, by immunofluorescence, colocalization of kinesin, microtubules, and membrane-bound organelles in mammalian cells and squid axoplasm (*8*−*11*). In addition, suppression of kinesin expression in cultured mammalian neurones using antisense oligonucleotides resulted in reduced neurite outgrowth due to decreased kinesin-mediated transport of axonal proteins to the neurite tip (*12*).

The quaternary structure of purified native kinesin is that of a tetrameric protein consisting of two heavy chains of ∼120 kDa and two light chains of ∼65 kDa (*13*, *14*) with the heavy chain comprising the ATP and microtubule-binding sites (*13*, *15*, *16*). Electron microscopic studies of antibody-coated kinesin revealed a three-domain structure for heavy chain consisting of a globular head linked via a rod domain to a fan-shaped tail containing bound light chain (*17*, *18*). Subsequent sequence analyses of kinesin heavy chain (KHC)[1] cDNA from various sources including *Drosophila* (*19*), squid (*20*), sea urchin (*21*), mouse (Genbank accession number X61435), and human (*22*, *23*) support this three-domain structure. The globular N-terminal motor domain contains the ATP and microtubule-binding sites (*24*, *25*) and has a similar crystal structure to the motor domains of both myosin and the kinesin-related protein ncd (*26*, *27*). The rodlike stalk domain consists of a long α-helical heptad repeat region which mediates dimerization between heavy chains through a coiled-coil interaction (*28*), while the small globular C-terminal domain is thought to be responsible for binding to light chain (*18*) and membranes (*29*). The membrane anchor for kinesin is believed to be kinec-

† This research was supported by Australian National Health and Medical Research Council Grant 960855.

* To whom correspondence should be addressed at the Centre for Virus Research, Westmead Institutes of Health Research, Westmead Hospital, Westmead, NSW 2145, Australia. Phone: 61-2-9845-6138. Facsimile: 61-2-9845-8300. E-mail: russelld@westgate.wh.usyd.edu.au.

‡ Westmead Institutes of Health Research.

§ Department of Biochemistry, University of Sydney.

|| School of Biological Sciences, University of Sydney.

[1] Abbreviations: CD, circular dichroism; KHC, kinesin heavy chain; KLC, kinesin light chain; uKHC, ubiquitous KHC; PCR, polymerase chain reaction; HisKHC, oligohistidine-tagged uKHC fragments; SDS−PAGE, sodium dodecyl sulfate−polyacrylamide gel electrophoresis; ECL, enchanced chemiluminescence; TBS, Tris-buffered saline; PVDF, poly(vinylidene difluoride).

10.1021/bi981163r CCC: $15.00
Published on Web 11/06/1998

tin, an endoplasmic reticulum transmembrane receptor (*30*−*33*).

Kinesin light chain (KLC) may regulate either KHC mechanochemical activity (*34*) or attachment of KHC to membrane cargo (*11*, *35*). Structural analysis of KLC cDNA from mammalian and invertebrate sources revealed a three-domain structure (*35*−*40*). The central and C-terminal domains of KLC consist of imperfect helical tandem repeats, joined by linkers, which are predicted to interact with membrane vesicles (*41*). Monoclonal antibody to the central domain tandem repeats of rat KLC inhibits axonal transport by displacing kinesin from membrane vesicles, demonstrating a direct role of light chain in binding kinesin to cargo (*11*). KLC isoforms which vary at the C-terminus arise from alternative splicing, and this heterogeneity may serve to target kinesin to specific vesicle receptors (*35*, *36*, *39*, *42*). The recent generation of transgenic *Drosophila* lacking functional KLC has directly demonstrated an essential role for KLC in axonal transport (*43*). The precise function of KLC though has yet to be clearly defined.

The N-terminal domain of KLC consists of several contiguous heptad repeats, which like heavy chain are predicted to form an α-helical coiled-coil structure. This region has been suggested to play a role in light chain dimerization and/or binding to heavy chain (*35*, *38*). In the case of *Drosophila* KLC, this heptad repeat region was shown to bind to a stalk−tail construct of KHC, with a predicted coiled-coil interaction presumably mediated through heptad repeats (*38*). This interaction was resistant to high salt and nonionic detergents, typical of a coiled-coil interaction, and would explain the noncovalent, high-affinity association of light and heavy chains observed with purified native kinesin (*13*, *14*).

In this study we have further examined the interaction of kinesin heavy and light chains to establish whether the stalk or tail domain of heavy chain binds light chain. We have focused on human rather than *Drosophila* kinesin since structural studies on kinesin from mammalian sources will allow establishment of relevant in vivo models, such as generation of transgenic mice, to test kinesin function. In particular, knowledge of the precise interaction of kinesin heavy and light chain will facilitate studies to determine the function of each chain in targeting and binding membrane organelles. Our results show that the binding site for human KLC in human ubiquitous KHC (uKHC; *22*) maps to amino acid residues 771−813, a region of KHC which corresponds to the C-terminus of the stalk domain. This heptad-repeat region, which is highly conserved between mammalian and invertebrate species, most likely forms an α-helical coiled-coil interaction with the N-terminus of KLC, a corresponding heptad-repeat region.

EXPERIMENTAL PROCEDURES

Human uKHC Expression Constructs. Fragments of human uKHC cDNA, corresponding to amino acid residues 555−963 (1.2 kb) and 771−963 (0.6 kb), inserted into the *Bam*HI site of the vector pGEX-2T were provided by Dr. Ron Vale, University of California, San Francisco. These fragments were generated by PCR using one of two 5′-primers, 5′-TAAGGATCCATGGCATCTTTACTAAAA-3′, containing codons 555−560, or 5′-TAAGGATCCATGCAAGATAGACGAGAA-3′, containing codons 771−776, both of which contained a *Bam*HI site (underlined). The 3′-primer used for PCR, 5′-CTCGGATCC**TTA**CACTTGTTTGCCTCC-3′, contained codons 959−963, the stop codon (bold), and a *Bam*HI site (underlined). Correct orientation of uKHC PCR fragments inserted into the *Bam*HI site of pGEX-2T was confirmed with *Sma*I digestion.

The following N-terminal oligohistidine-tagged uKHC constructs were generated from these pGEX-2T constructs: 555−963, 555−876, 771−963, 771−876, and 855−963 (uKHC amino acid numbering). First, the entire 1.2 or 0.6 kb *Bam*HI fragments containing uKHC from pGEX-2T were inserted into the *Bam*HI site of vector pET-28a. Orientation was confirmed by an internal *Bgl*II site in the uKHC fragments. In addition, 0.96 kb *Bam*HI−*Hin*dIII (amino acids 555−876) and 0.33 kb *Bgl*II−*Eco*RI (amino acids 855−963) fragments of pGEX2T/uKHC555−963 were inserted into pET-28a and pET-28b, respectively. To generate pET-28a/uKHC771−876, pET-28a/uKHC771−963 was digested with *Hin*dIII to remove a 0.3 kb fragment and the ends religated. pET-28a/uKHC555−772 and pET-28a/uKHC771−813 were generated by PCR using pET-28a/uKHC555−963 as template and Vent DNA polymerase (NEB). The 5′-primer in each case was the T7 promoter sequencing primer. The 3′-primer for uKHC555−772, 5′-GCGAAT**TCA**TTGCATAACCGTAAGTTCATG-3′, contained codons 766−772, the stop codon (bold), and an *Eco*RI site (underlined). The 3′-primer for uKHC555−813, 5′-GCGAAT**TCA**CTTTTTAACTCTTGTAGCCAG-3′, contained codons 807−813, the stop codon (bold), and an *Eco*RI site (underlined). PCR products were digested with *Xba*I and *Eco*RI prior to ligation into pET-28a.

Human KLC Expression Constructs. Human KLC cDNA was provided by Dr. Yofre Cabeza-Arvelaiz, Baylor College of Medicine, Houston, TX, as plasmid pPL.Mu.KLC (*37*). KLC cDNA was removed from this plasmid as a 2 kb *Nco*I−*Bam*HI fragment and inserted into pET-28a. The resulting expression construct, termed pET-28a/KLC, lacked the oligohistidine fusion tag and encoded residues 4−569. pET-28a/KLC was then used to generate pET-28a/KLC4−363 and pET-28a/KLC4−15/364−569. First, pET-28a/KLC was digested with *Xho*I (to remove a 0.95 kb fragment of the KLC insert) and the 5′ overhangs filled in with Klenow polymerase prior to blunt end ligation. A stop codon was provided in-frame by the vector. The resulting construct, pET-28a/KLC4−363, lacked the C-terminal third of KLC. The construct, pET-28a/KLC4−15/364−569, was generated by digesting pET-28a/KLC with *Bgl*II (filled-in) and *Xho*I to liberate a 0.95 kb fragment containing the C-terminal end of KLC. This fragment was religated to pET-28a/KLC which had been digested with *Hin*dIII (filled-in) and *Xho*I to remove essentially all of the 2 kb KLC insert. The new KLC insert now coded for residues 4−15 and 364−569. All KHC and KLC constructs were sequenced at the 5′ and 3′ insert/vector junctions using T7 terminator and promoter sequencing primers. In addition, PCR products were completely sequenced.

Expression of Recombinant uKHC and KLC. Oligohistidine fusion constructs were expressed in *Escherichia coli* strain BL21(DE3). Bacteria were grown in Luria broth with 50 μg/mL kanamycin sulfate to mid-log phase at 37 °C prior to induction of recombinant protein expression with 1 mM

isopropyl β-D-thiogalactopyranoside for 3 h at 30 °C. Typically 100 mL induced bacterial cultures were harvested by centrifugation at 4 °C (2500*g* for 10 min). The cell pellet was resuspended in 5 mL of lysis buffer [20 mM Tris-HCl, pH 7.9, 5 mM imidazole, 1 mM phenylmethylsulfonyl fluoride, 2 μg/mL leupeptin, 0.1% (v/v) Triton X-100, and 500 mM NaCl] and then lysed by sonication. Insoluble material was removed by centrifugation at 4 °C (10000*g* for 20 min), and the soluble fraction was used for binding assays.

Purification of uKHC and KLC Complexes. Complexes of uKHC and KLC were reconstituted using oligohistidine-tagged uKHC (HisKHC) fragments bound to His-bind resin (Novagen; charged with 50 mM nickel sulfate) to act as an affinity column for KLC. Typically 50 μL of beads, equilibrated with binding buffer (20 mM Tris-HCl, pH 7.9, 5 mM imidazole, 500 mM NaCl), was added to 1 mL of bacterial lysate containing HisKHC fragments and incubated with rocking for 3 h at 4 °C. Beads were then washed with 3 × 20 volumes of wash buffer (20 mM Tris-HCl, pH 7.9, 120 mM imidazole, 500 mM NaCl) prior to addition of 1 mL of bacterial lysate containing KLC. Beads were incubated overnight with rocking at 4 °C and washed as above, and the bound proteins were eluted by incubating with 50 μL of elution buffer (20 mM Tris-HCl, pH 7.9, 1 M imidazole, 500 mM NaCl) for 1 h at 4 °C.

Analysis of Purified uKHC and KLC Complexes. Protein samples were separated by 14% SDS−PAGE (*44*) under reducing conditions. For immunoblotting (*45*), proteins were then electroblotted to a Hybond-ECL nitrocellulose membrane (Amersham) at 50 mA, overnight. Membrane strips containing unstained molecular weight markers were removed and stained with 0.1% (w/v) amido black. The remainder of the membrane was blocked for 1 h at room temperature with 5% (w/v) skim milk powder in Tris-buffered saline (TBS)−0.1% (v/v) Tween 20, washed several times with TBS−0.1% Tween 20, and then incubated for 1 h with primary antibody in 1% (w/v) skim milk powder in TBS−0.1% Tween 20. Rabbit polyclonal anti-human uKHC stalk region 523−773 (*23*) and anti-squid KHC, cross-reactive with mammalian KHCs (*22*), were provided by Dr. Ron Vale, University of California, San Francisco. The other primary antibodies used included mouse monoclonal anti-bovine KLC L1 and L2 (Chemicon Chemical Co.), cross-reactive with mammalian KLCs (*8*), diluted 1:5000. The blot was again washed with TBS−0.1% Tween 20 prior to application of the secondary antibody, goat anti-rabbit IgG (Pierce) or sheep anti-mouse IgG (Amersham) conjugated to horseradish peroxidase, diluted 1:200 000 and 1:10 000, respectively, in 1% (w/v) skim milk powder in TBS−0.1% Tween 20. Incubation and wash were the same as for primary antibody. Antibody binding was detected on X-ray film as chemiluminescence generated with Supersignal substrate (Pierce, Rockford, IL).

For N-terminal protein sequencing of KLC, samples were electroblotted to a Hybond-PVDF membrane (Amersham) and stained with 0.025% (w/v) Coomassie Blue R-250 in the absence of acetic acid. Minor modifications of the SDS−PAGE and blotting procedures were introduced to reduce blocking of the N-terminus prior to sequencing (*46*).

Circular Dichroism Spectroscopy. The circular dichroism (CD) spectra in the far-UV region were recorded on a Jasco J-720 spectropolarimeter. Spectra were recorded with a 1 mm path length cell, maintained at 25 °C. The instrument was calibrated with *d*-10-(+)-camphorsulfonic acid (0.06% w/v) at 290.5 nm. Spectral data were collected in a solution of 5 mM NaH_2PO_4, pH 7.4, at 0.5 nm intervals from 184 to 260 nm at a protein concentration of 0.09 mg/mL with the average of 10 scans reported. The percent α-helical content was calculated from data using the variable selection method (*47*, *48*). Protein concentration was determined by amino acid analysis.

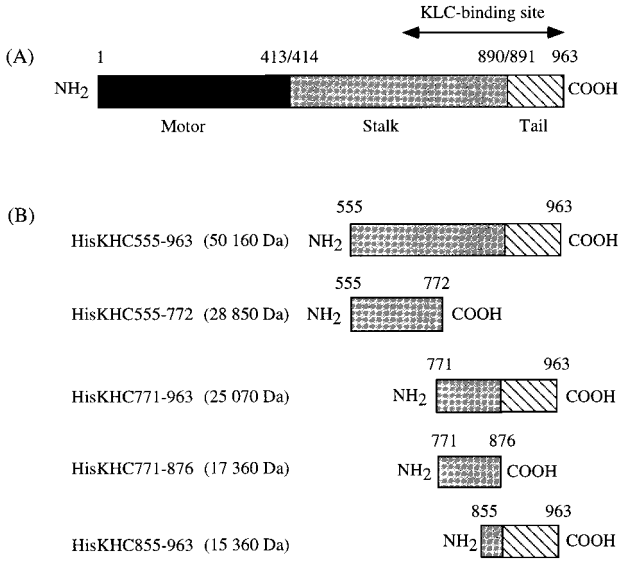

FIGURE 1: Schematic representation of human uKHC fragments initially expressed in this study. (A) Human uKHC consists of a motor, stalk, and tail domain (*22*). The motor domain contains the ATP- and microtubule-binding sites as well as a C-terminal neck region that mediates motor domain dimerization; the rodlike stalk provides additional sites of heavy chain dimerization, while the globular tail anchors the heavy chain to membranes. The region (664−963) which binds KLC is highlighted. (B) HisKHC555−963 to HisKHC855−963 represent the fragments of human uKHC initially expressed in this study as oligohistidine N-terminally tagged bacterial fusion proteins (chosen on the basis of the known KLC-binding region in KHC). Predicted molecular masses of the fusion proteins are given in parentheses, and the numbers above each diagram correspond to the amino acid numbering of human uKHC.

RESULTS

Identification of the KLC-Binding Site in uKHC. In this study we initially expressed in bacteria several fragments of the heavy chain of ubiquitous human kinesin as fusion proteins tagged at the N-terminus with a hexameric oligohistidine sequence. These fragments span amino acid residues 555−963 of human uKHC (*22*), a region that corresponds to the majority of the stalk domain and all of the tail domain of KHC but excludes the motor domain (Figure 1). This region was chosen to ascertain whether the binding site for KLC in KHC resides in the stalk or tail domain. Previous results observed with *Drosophila* kinesin showed that a stalk−tail glutathione-*S*-transferase fusion construct of heavy chain, lacking the motor domain, still bound light chain (*38*). This stalk−tail construct contained amino residues 688−975 (*Drosophila* KHC numbering) which are equivalent to residues 664−963 of human uKHC (Figure 1).

These HisKHC fragments were then used in an in vitro reconstitution assay to ascertain their ability to bind KLC.

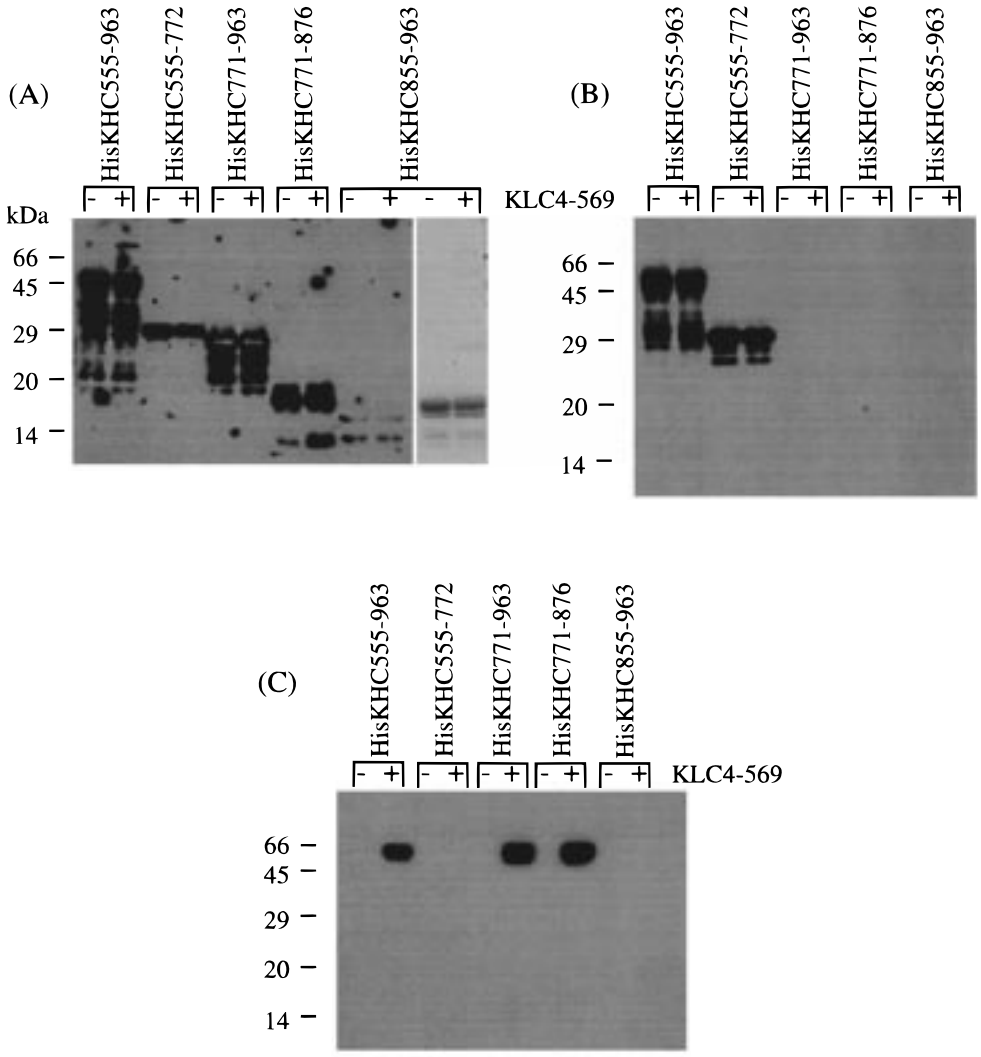

FIGURE 2: Identification of KLC complexed with oligohistidine-tagged uKHC fragments. HisKHC fragments were bound to Ni^{2+}-charged beads prior to addition of a bacterial lysate containing KLC4−569. HisKHC/KLC complexes were then eluted with imidazole prior to separation by 14% SDS−PAGE under reducing conditions and immunoblotting with various antibodies. (A) The presence of each eluted HisKHC fragment was ascertained by probing with rabbit anti-squid KHC, cross-reactive with mammalian KHCs (*22*). The presence of HisKHC855−963 had to be confirmed by staining with Coomassie Blue (last two lanes). (B) Rabbit antibody against human uKHC stalk region 523−773 (*23*) confirmed the presence of this region in the correct HisKHC fragments, HisKHC555−963 and HisKHC555−772. (C) Mouse anti-KLC, cross-reactive with mammalian KLCs and directed to the C-terminus of KLC (*8*), showed KLC4−569 bound to HisKHC555−963, HisKHC771−963, and HisKHC771−876.

Since the binding of KLC to KHC was predicted to be an α-helical coiled-coil interaction (*38*), the assay was carried out in conditions of high salt (0.5 M) which do not affect such interactions but do decrease electrostatic interactions. Expressed HisKHC fragments in bacterial lysates were immobilized, via their oligohistidine tag, on Ni^{2+}-charged beads and tested for their ability to bind recombinant untagged KLC (residues 4−569), referred to as KLC4−569, in bacterial lysates. Complexes formed on beads were eluted, separated by SDS−PAGE, and immunoblotted.

The presence of eluted HisKHC fragments was confirmed using two rabbit polyclonal anti-KHC antibodies. The first antibody was anti-squid KHC, affinity-purified using bovine KHC (*22*), which detected all of the expressed, eluted HisKHC fragments (see Figure 1B for predicted molecular masses) with some observed proteolysis (Figure 2A). HisKHC855−963, though, exhibited only a weak signal at its predicted mobility of 16 kDa. This region is very homologous between species, and such weak reactivity could indicate that it is poorly immunogenic. Detection by Coomassie Blue R-250 staining did confirm the presence of eluted HisKHC855−963 (Figure 2A, last two lanes). The second antibody was against part of the stalk region (residues 523−773) of human uKHC (*23*), and, as expected, HisKHC555−963 and HisKHC555−772 were detected with this antibody while HisKHC771−963, HisKHC771−876, and HisKHC855−963 were not detected (Figure 2B).

Immunoblotting using mouse monoclonal anti-bovine KLC antibody L2, which reacts with the C-terminus of KLC (*8*), detected the presence of KLC4−569 coeluting with various HisKHC fragments (Figure 2C). KLC4−569 bound to HisKHC555−963, HisKHC771−963, and HisKHC771−876 but did not bind to HisKHC555−772 or HisKHC855−963 (Figure 2C). This indicates that the minimal KHC fragment required to bind KLC4−569 was 771−876, a region common to all KLC-binders. The band at 65 kDa (the predicted molecular mass of expressed KLC4−569) was not detected by either anti-KHC antibody (Figure 2A,B) and was only present in HisKHC fragments incubated with lysates containing KLC4−569 (Figure 2C). In addition, N-terminal protein

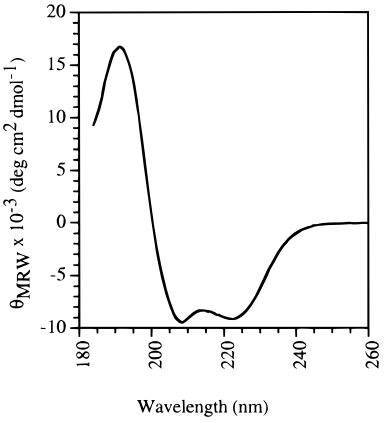

FIGURE 3: CD spectrum of HisKHC771−963. Spectral data was collected in a solution of 5 mM NaH_2PO_4, pH 7.4, at a protein concentration of 0.09 mg/mL.

sequencing of this 65 kDa band eluting with HisKHC771−876 gave two sequences, VYIKE and MVYIK, with more of the former. Based on the KLC cDNA used for expression, the protein sequence should start at the second methionine residue (position 4) and be MVYIKE (*37*). This conclusively identifies the bound protein to be human KLC and highlights that there was some loss of the initiating methionine during bacterial expression.

Secondary Structure of the Light Chain-Binding Site. CD spectroscopy was used to determine the secondary structure content of recombinant HisKHC771−963 which contains the binding site for KLC. Similar measurements were unable to be carried out on the minimal KLC-binding domain HisKHC771−876 as this fragment was insoluble in the buffer chosen for CD measurements. The far-UV CD spectrum of HisKHC771−963 shows a characteristic α-helical spectrum with a maximum at 192 nm and double minima at 208 and 222 nm (Figure 3). The spectrum corresponds to an α-helical content of ∼70%, which compares favorably with an α-helical content of 54% predicted by the method of Chou and Fasman (*49*), i.e., 121 residues out of 227 residues (includes 34 residues at the N-terminus coded by pET-28a). Of these predicted α-helical residues, 116 (or 96%) have a greater than 94% probability of forming an α-helical coiled-coil structure, as determined using the program Macstripe (*50*) which employs the Lupas algorithm (*51*).

Further Characterization of the KLC-Binding Site in uKHC. Alignment of the KLC-binding region (771−876) of human uKHC with the equivalent regions of mammalian and invertebrate KHCs highlights that this region is highly conserved (Figure 4). In particular, there are two subdomains which contain heptad repeats that are predicted to form an α-helical coiled-coil structure (Figure 4). To determine which domain is the most important for binding KLC, the following constructs were generated: HisKHC555−876 (contains both subdomains) and HisKHC555−813 (contains only subdomain 1). Both these constructs contain the non-KLC binding region 555−772 (Figure 5A,B) which was used as a negative control. To help confirm the specificity of the KHC/KLC interaction, additional untagged KLC constructs were also generated. These included N-terminal, KLC4−363, and C-terminal, KLC4−15/364−569, fragments of KLC4−569 (Figure 5C). On the basis of work with

```
                                Subdomain 1
          defg abcdefg abcdefg abcdefg abcdefg a
HU   771 MQDR REQARQD LKGLEET VAKELQT LHNLRKL FVQDLATRVKK----SA
HN   769 LYE* H**SK** ******* **R**** ******* ****VT*****----**
M    769 LYE* H**SK** ******* **R**** ******* ****VT*****----**
D    792 TNE* *****K* *****D* ******* ******* *****QQ*IR*NV--VN
S    769 QI** ****K** ******* ******* ******* *****QNK***SCSKTE
U    766 QF** ****K** ******* ******* ******* **S**QN****----AL

                                                    Subdomain 2
                          bcdefg abcdefg abcdefg abcdefg abcdefg ab
HU   816 E--IDSDDTGG SAAQKQK ISFLENN LEQLTKV HKQLVRD NADLRCE LP
HN   814 *--MEPE*S** IHS**** ******* ******* ******* ******* **
M    814 *--MEPE*S** IHS**** ******* ******* ******* ******* **
D    839 *---ESEED** *L***** ******* *D***** ******* ******* **
S    818 *---EDE**** N****** ******* ******* ******* ******* **
U    811 *GGDRD**S** *Q***** ******* ******* ******* ******* **

          cdefg abcdefg abc
HU   862 KLEKR LRATAER VKA
HN   860 ***** ******* ***
M    860 ***** ******* ***
D    884 ***** **C*M** ***
S    863 ***** ****M** **S
U    859 ***R* ****S** ***
```

FIGURE 4: Alignment of the KLC-binding site of human uKHC (residues 771−876) with the corresponding regions of mammalian and invertebrate KHC protein sequences. Protein sequences (one-letter code) compared to human uKHC (HU) include human neuronal (HN), mouse (M), *Drosophila* (D), squid (S), and sea urchin (U) KHCs (*21*−*25*). Amino acid numbering is given in the left margin. Identical residues are represented by an asterisk while a line indicates gaps introduced to maximize alignment. The probability that human uKHC region 771−876 would form an α-helical coiled-coil structure and therefore contain characteristic heptad repeats was determined using the program Macstripe (*50*) which employs the Lupas algorithm (*51*). Heptad repeats are indicated as *abcdefg* where *a* and *d* are predominantly hydrophobic residues and form the core of the predicted coiled-coil amphipathic helix. Only those residues with a probability of greater than 94% of forming a coiled-coil structure are indicated.

Drosophila (*38*), residues 30−185 at the N-terminus of human KLC should contain the binding site for KHC; therefore, only the N-terminal KLC fragment should bind KHC.

The results of in vitro reconstitution of HisKHC555−772, HisKHC555−813, and HisKHC555−876 with each of the three untagged KLC fragments were again assessed by immunoblotting. As expected, all the KHC fragments were detected by the anti-stalk KHC antibody, since each has in common region 555−772 (Figure 6A). KLC binding to these uKHC fragments was assessed using two monoclonal anti-KLC antibodies, L1 and L2. L1, which binds within the first 50 amino acids of KLC (*11*), was used to detect KLC4−569 and N-terminal KLC4−363. Both of these KLC fragments were observed bound to HisKHC555−876 and HisKHC555−813 (Figure 6B). L2, which binds to the C-terminus of KLC (*8*, *11*, *18*), was used to detect KLC4−569 and C-terminal KLC4−15/364−569. Only KLC4−569 was shown to bind to HisKHC555−876 and HisKHC555−813 (Figure 6C). The presence of expressed KLC4−15/364−569 in bacterial lysates added to uKHC fragments was confirmed using antibody L2 (Figure 6D). Its confirmed presence in lysates indicates that the absence of binding to uKHC fragments was not due to lack of expression in bacteria. These results further define the KLC-binding site in uKHC to region 773−813 which contains subdomain 1

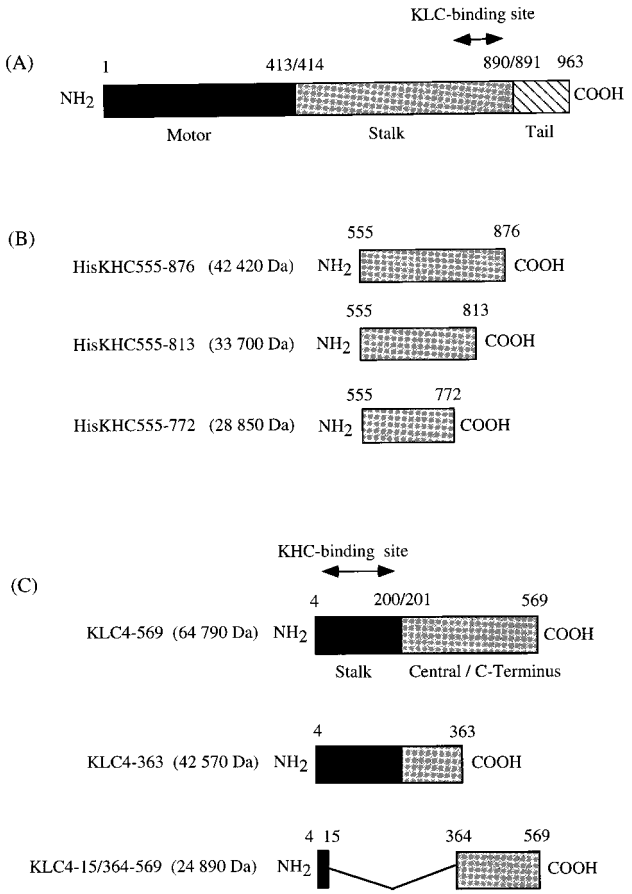

FIGURE 5: Schematic representation of additional human uKHC and KLC fragments expressed in this study. (A) The position of the KLC-binding site in uKHC (residues 771−876), as determined in this study, is highlighted. (B) Oligohistidine-tagged uKHC truncations of the KLC-binding site. (C) Untagged KLC fragments. Human KLC consists of a stalk domain which contains the binding site for uKHC (residues 30−185) and a central/C-terminal domain which is predicted to bind to organelles (*41*). Predicted molecular masses of the fusion proteins are given in parentheses, and the numbers above each diagram correspond to amino acid numbering.

(Figure 4) and also confirm that the N-terminus of KLC contains the uKHC-binding site.

DISCUSSION

The cloning of both the heavy and light chains of kinesin in recent years has led to numerous structure−function studies on this heterotetrameric motor protein. These studies have concentrated mainly on the heavy chain N-terminal motor domain with little emphasis on the light chain and the nature of its known interaction with the C-terminal end of the heavy chain (*17*, *18*). The possibility of recombinantly expressing separate kinesin heavy and light chains facilitates the study of their interaction by in vitro reconstitution. Previously, this has been not been possible since the chains of purified native kinesin, though interacting noncovalently, are extremely difficult to separate without the aid of denaturing agents (*13*, *14*). To date though there has only been one reported study using recombinant expression and in vitro reconstitution of kinesin chains to map the interaction of KLC to the stalk−tail region of *Drosophila* KHC. The nature of the interaction was postulated to be that of an α-helical coiled-coil mediated via heptad-repeat regions in each chain (*38*).

In vitro reconstitution of recombinant human kinesin was employed in this study to more precisely define the KLC-binding site in KHC. High ionic strength was chosen for the assay since the predicted hydrophobic α-helical coiled-coil interaction would not be affected by such conditions. Analysis was initially based on the reconstitution of the following recombinantly expressed oligohistidine-tagged fragments of human uKHC with KLC: 555−963, 555−772, 771−963, 771−876, 855−963 (amino acid numbering). Assessment of the binding of these fragments to recombinantly expressed untagged KLC (Figure 2) mapped the KLC-binding site to the heptad repeat containing fragment 771−876 of uKHC. This region which corresponds to the C-terminal end of the heavy chain stalk domain, was common to the other identified light chain-binding fragments 555−963 and 771−963 but only partially represented in the nonbinder 855−963 (Figure 1). This supports the previous findings for *Drosophila* kinesin which indicated that the light chain binds to a heavy chain stalk−tail construct equivalent to residues 664−963 of uKHC (*38*). We have taken this finding a step further to now exclude the tail domain (Figure 1, residues 891−963) as a site for light chain binding via heptad repeats since heavy chain fragment 855−963, incorporating the tail domain, fails to bind to light chain at high ionic strength. This is not unexpected as the tail domain has been implicated as the site for organelle receptor binding (*29*) and it would be hard to envisage cobinding of light chain.

A number of observations in this study suggest that the nature of the interaction of KLC with KHC appears to be that of an α-helical coiled-coil. First, KHC region 771−876 identified initially in this study as the KLC-binding site has a high probability of forming an α-helical coiled-coil as evidenced by the presence of two subdomains that contain the characteristic heptad repeat required for the formation of an α-helical coiled-coil amphipathic helix (Figure 4; *51*). These regions of conventional human uKHC are highly conserved across mammalian and invertebrate sources particularly at the position of the helix core residues (*a* and *d*) which suggests evolutionary pressure to maintain this region as an important functional site, in this case binding of light chain (Figure 4). CD spectroscopy of HisKHC771−963 gave an α-helical content of around 70%, which most likely points to region 771−876 as being α-helical in nature. This is because the majority of the predicted α-helical content (>90%) aligns with the heptad repeats which are contained within region 771−908 of uKHC.

Extended analysis of the KHC/KLC interaction using the constructs HisKHC555−876, HisKHC555−813, and HisKHC555−772 indicated that deletion of residues 814−876 had no apparent quantitative effect on binding of KLC (Figure 6). This indicates that within 771−876, region 773−813 or subdomain 1 contains the principal KLC-binding site. This region itself has 4 contiguous heptad repeats (775−802) that are highly conserved, with 22 out of 28 residues identical, while 3 out of the remaining 6 residues are conservative changes (Figure 4).

Further evidence for an α-helical coiled-coil interaction comes from the fact that the N-terminal stalk domain of *Drosophila* KLC, which is equivalent to residues 1−200 of human KLC, contains the binding site for KHC and like region 775−802 in human KHC consists of several heptad

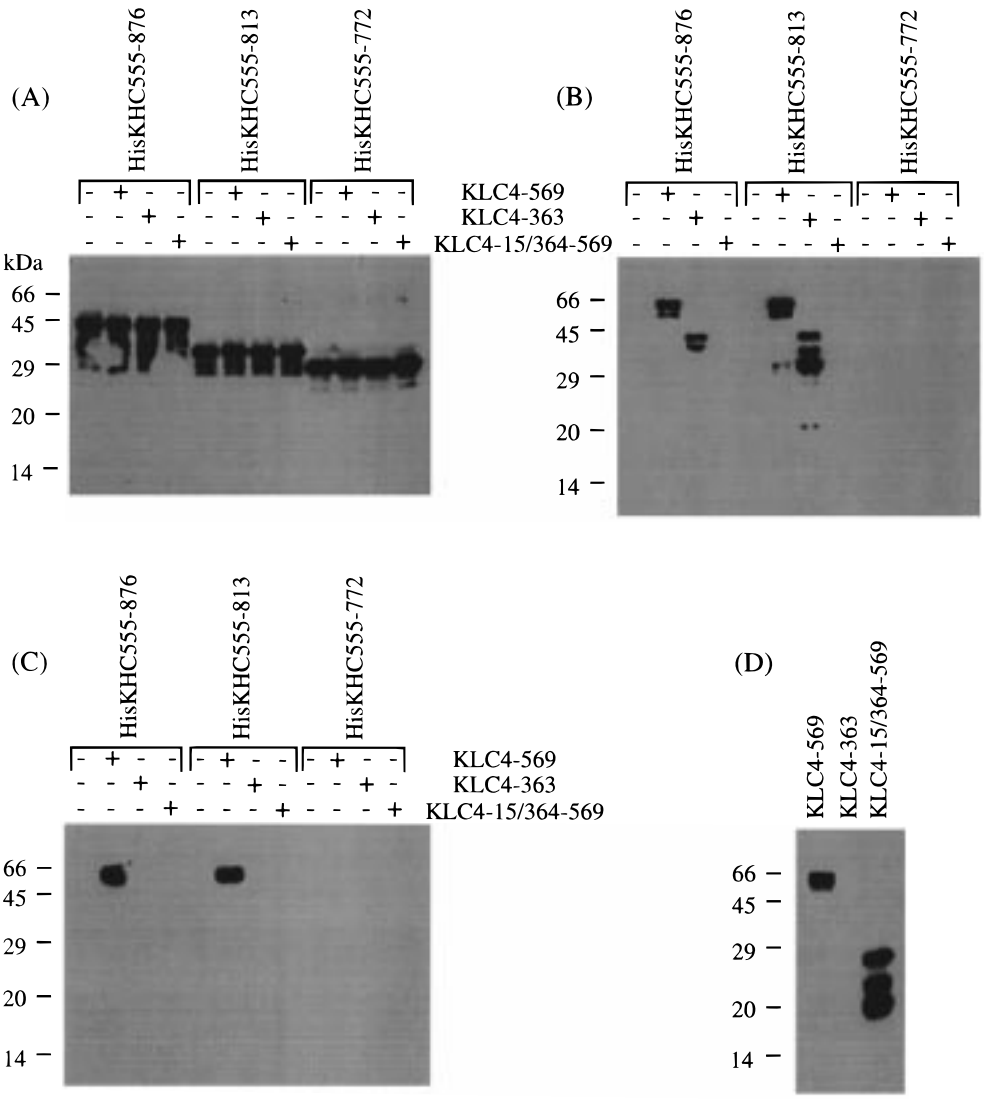

FIGURE 6: Identification of KLC fragments complexed with subdomains of the KLC-binding site (771−876) of uKHC. HisKHC fragments were bound to Ni^{2+}-charged beads prior to addition of a bacterial lysate containing either essentially full-length KLC (KLC4−569), an N-terminal KLC fragment (KLC4−363), or a C-terminal KLC fragment (KLC4−15/364−569). HisKHC/KLC complexes were then eluted with imidazole prior to separation by 14% SDS−PAGE under reducing conditions and immunoblotting with various antibodies. (A) The presence of each eluted HisKHC fragment was confirmed by probing with rabbit antibody against human uKHC stalk region 523−773 (*23*). (B) Mouse anti-KLC, cross-reactive with mammalian KLCs and directed to the N-terminus of KLC (*8*), showed KLC4−569 and KLC4−363 bound to both HisKHC555−876 and HisKHC555−813. (C) Mouse anti-KLC, cross-reactive with mammalian KLCs and directed to the C-terminus of KLC (*8*), again identified KLC4−569 bound to HisKHC555−876 and HisKHC555−813. KLC4−15/364−569 was not detected with any of the HisKHC fragments. As expected, this antibody did not detect KLC4−363. (D) The C-terminal anti-KLC antibody was then used to verify the presence of KLC4−15/364−569 in bacterial lysates added to HisKHC fragments. Bacterial lysates containing KLC4−569 and KLC4−363 served as positive and negative controls, respectively.

repeats (*38*). To support this, evidence is presented in this study for selective interaction of KHC region 775−802 (within the fragment 773−813) with an N-terminal fragment of human KLC spanning residues 4−363 (Figure 6). The heptad repeat regions as predicted by the method of Lupas (*51*) are only in the N-terminus of KLC and in the case of human KLC range from residues 28−55 and 87−152. From studies with *Drosophila* KLC (*38*), it can be inferred that region 28−55 is not the KHC-binding site as a construct spanning the equivalent of residues 1−104 of human KLC did not bind KHC. Therefore, it is likely that region 105−152 contains the uKHC-binding site.

Finally, in both our study and that conducted with *Drosophila* kinesin (*38*), the interaction of heavy and light chain was unaffected by high ionic strength. Taken together these observations are consistent with human KHC region 775−802 and human KLC region 105−152 interacting via heptad-repeat regions to form a double-stranded amphipathic helix stabilized predominantly by a hydrophobic core.

This study has shown for the first time in humans the nature of the interaction of KLC with uKHC. We now plan to alter both region 775−802 of uKHC and region 105−152 of KLC by site-directed mutagenesis, targeting heptad repeat core residues (*a* and *d*), to establish that these sites do in fact form an α-helical coiled-coil structure. This will also identify which are the most important heptad regions for interaction. Furthermore, peptides spanning both these regions will be synthesized and the nature of their interaction assessed using both CD and analytical sedimentation equilibrium to establish secondary structure, affinity, and stoichiometry of the KHC/KLC complex. It should then be possible to reconstitute in vivo a KHC/KLC complex with

reduced affinity and gain insight into the effects on kinesin activity and the precise role of light chain in the targeting and binding of heavy chain to membrane organelles.

ACKNOWLEDGMENT

We thank the individuals indicated in the text for their generous provision of reagents especially Professor Ron Vale (Department of Cellular and Molecular Pharmacology, University of California). This research has been facilitated by access to the Australian Proteome Analysis Facility established under the Australian Government's Major National Research Facilities Program. This facility performed N-terminal protein sequencing and amino acid analysis. DNA sequencing was carried out by Mark Wheeler at the DNA sequence and synthesis facility, Westmead Institutes of Health Research, Westmead Hospital.

REFERENCES

1. Vale, R. D., Reese, T. S., and Sheetz, M. P. (1985) *Cell 42*, 39−50.
2. Vale, R. D., Schnapp, B. J., Mitchison, T., Steuer, E., Reese, T. S., and Sheetz, M. P. (1985) *Cell 43*, 623−632.
3. Brady, S. T. (1985) *Nature 317*, 73−75.
4. Scholey, J. M., Porter, M. E., Grissom, P. M., and McIntosh, J. R. (1985) *Nature 318*, 483−486.
5. Kuznetsov, S. A., and Gelfand, V. I. (1986) *Proc. Natl. Acad. Sci. U.S.A. 83*, 8530−8534.
6. Porter, M. E., Scholey, J. M., Stemple, D. L., Vigers, G. P., Vale, R. D., Sheetz, M. P., and McIntosh, J. R. (1987) *J. Biol. Chem. 262*, 2794−2802.
7. Wagner, M. C., Pfister, K. K., Bloom, G. S., and Brady, S. T. (1989) *Cell Motil. Cytoskeleton 12*, 195−215.
8. Pfister, K. K., Wagner, M. C., Stenoien, D. L., Brady, S. T., and Bloom, G. S. (1989) *J. Cell Biol. 108*, 1453−1463.
9. Brady, S. T., Pfister, K. K., and Bloom, G. S. (1990) *Proc. Natl. Acad. Sci. U.S.A. 87*, 1061−1065.
10. Hirokawa, N., Sato-Yoshitake, R., Kobayashi, N., Pfister, K., Bloom, G., and Brady, S. (1991) *J. Cell Biol. 114*, 295−302.
11. Stenoien, D. L., and Brady, S. T. (1997) *Mol. Biol. Cell 8*, 675−689.
12. Ferreira, A., Niclas, J., Vale, R. D., Banker, G., and Kosik, K. S. (1992) *J. Cell Biol. 117*, 595−606.
13. Bloom, G. S., Wagner, M. C., Pfister, K. K., and Brady, S. T. (1988) *Biochemistry 27*, 3409−3416.
14. Kuznetsov, S. A., Vaisberg, E. A., Shanina, N. A., Magretova, N. N., Chernyak, V. Y., and Gelfand, V. I. (1988) *EMBO J. 7*, 353−356.
15. Kuznetsov, S. A., Vaisberg, Y. A., Rothwell, S. W., Murphy, D. B., and Gelfand, V. I. (1989) *J. Biol. Chem. 264*, 589−595.
16. Ingold, A. L., Cohn, S. A., and Scholey, J. M. (1988) *J. Cell Biol. 107*, 2657−2667
17. Amos, L. A. (1987) *J. Cell Sci. 87*, 105−111.
18. Hirokawa, N., Pfister, K. K., Yorifuji, H., Wagner, M. C., Brady, S. T., and Bloom, G. S. (1989) *Cell 56*, 867−878.
19. Yang, J. T., Laymon, R. A., and Goldstein, L. S. (1989) *Cell 56*, 879−889.
20. Kosik, K. S., Orecchio, L. D., Schnapp, B., Inouye, H., and Neve, R. L. (1990) *J. Biol. Chem. 265*, 3278−3283.
21. Wright, B. D., Henson, J. H., Wedaman, K. P., Willy, P. J., Morand, J. N., and Scholey, J. M. (1991) *J. Cell Biol. 113*, 817−833.
22. Navone, F., Niclas, J., Hom-Booher, N., Sparks, L., Bernstein, H. D., McCaffrey, G., and Vale, R. D. (1992) *J. Cell Biol. 117*, 1263−1275.
23. Niclas, J., Navone, F., Hom-Booher, N., and Vale, R. D. (1994) *Neuron 12*, 1059−1272.
24. Scholey, J. M., Heuser, J., Yang, J. T., and Goldstein, L. S. (1989) *Nature 338*, 355−357.
25. Yang, J. T., Saxton, W. M., Stewart, R. J., Raff, E. C., and Goldstein, L. S. (1990) *Science 249*, 42−47.
26. Kull, F. J., Sablin, E. P., Lau, R., Fletterick, R. J., and Vale, R. D. (1996) *Nature 380*, 550−555.
27. Sablin, E. P., Kull, F. J., Cooke, R., Vale, R. D., and Fletterick, R. J. (1996) *Nature 380*, 555−559.
28. De Cuevas, M., Tao, T., and Goldstein, L. S. (1992) *J. Cell Biol. 116*, 957−965.
29. Skoufias, D. A., Cole, D. G., Wedaman, K. P., and Scholey, J. M. (1994) *J. Biol. Chem. 269*, 1477−1485.
30. Toyoshima, I., Yu, H., Steuer, E. R., and Sheetz, M. P. (1992) *J. Cell Biol. 118*, 1121−1131.
31. Fütterer, A., Kruppa, G., Krämer, B., Lemke, H., and Krönke, M. (1995) *Mol. Biol. Cell 6*, 161−170.
32. Kumar, J., Yu, H., and Sheetz, M. P. (1995) *Science 267*, 1834−1837.
33. Yu, H., Nicchitta, C. V., Kumar, J., Becker, M., Toyoshima, I., and Sheetz, M. P. (1995) *Mol. Biol. Cell 6*, 171−183.
34. Hackney, D. D., Levitt, J. D., and Wagner, D. D. (1991) *Biochem. Biophys. Res. Commun. 174*, 810−815.
35. Cyr, J. L., Pfister, K. K., Bloom, G. S., Slaughter, C. A., and Brady, S. T. (1991) *Proc. Natl. Acad. Sci. U.S.A. 88*, 10114−10118.
36. Beushausen, S., Kladakis, A., and Jaffe, H. (1993) *DNA Cell Biol. 12*, 901−909.
37. Cabeza-Arvelaiz, Y., Shih, L. C., Hardman, N., Asselbergs, F., Bilbe, G., Schmitz, A., White, B., Siciliano, M. J., and Lachman, L. B. (1993) *DNA Cell Biol. 12*, 881−892.
38. Gauger, A. K., and Goldstein, L. S. (1993) *J. Biol. Chem. 268*, 13657−13666.
39. Wedaman, K. P., Knight, A. E., Kendrick-Jones, J., and Scholey, J. M. (1993) *J. Mol. Biol. 231*, 155−158.
40. Fan, J., and Amos, L. A. (1994) *J. Mol. Biol. 240*, 507−512.
41. Gindhart, J. G., Jr., and Goldstein, L. S. (1996) *Trends Biochem. Sci. 21*, 52−53
42. Khodjakov, A., Lizunova, E. M., Minin, A. A., Koonce, M. P., and Gyoeva, F. K. (1998) *Mol. Biol. Cell 9*, 333−343.
43. Gindhart, J. G., Jr., Desai, C. J., Beushausen, S., Zinn, K., and Goldstein L. S. B. (1998) *J. Cell Biol. 141*, 443−454.
44. Laemmli, U. K. (1970) *Nature 227*, 680−685.
45. Towbin, H., Staehelin, T., and Gordon, J. *Proc. Natl. Acad. Sci. U.S.A. 76*, 4350−4354.
46. Speicher, D. W. (1989) in *Techniques in Protein Chemistry*, pp 24−35, Academic Press, New York.
47. Compton, L. A., and Johnson, W. C., Jr. (1986) *Anal. Biochem. 155*, 155−167.
48. Manavalan, P., and Johnson, W. C., Jr. (1987) *Anal. Biochem. 167*, 76−85.
49. Chou, P. Y., and Fasman, G. D. (1978) *Annu. Rev. Biochem. 47*, 251−276.
50. Knight, A. E. (1994) The Diversity of Myosin-Like Proteins, Cambridge, U.K. (Ph.D. Thesis).
51. Lupas, A., Van Dyke, M., and Stock, J. (1991) *Science 252*, 1162−1164.

BI981163R